Optimization of Third-Order Intermodulation Product and Output Power from an *X*-Band MESFET Amplifier Using Volterra Series Analysis

GEORGE M. LAMBRIANOU AND COLIN S. AITCHISON

Abstract—**A third-order analysis for accurately predicting large-signal power and intermodulation distortion performance for GaAs MESFET amplifiers is presented. The analysis is carried out for both single- and two-tone input signals using the Volterra series representation and is based only on small-signal measurements. Simple expressions for the nonlinear power gain frequency response, the output power, the gain compression factor, and the third-order intermodulation (IM_3) power are presented. The major sources of gain compression and intermodulation distortion are identified. Based on the developed nonlinear analysis in conjunction with the device nonlinear model, a systematic procedure for designing a MESFET amplifier under large-signal conditions for optimum output power and IM_3 performance is proposed. The method utilizes out of band computed matching compensation through a nonlinear model of the amplifier. The accuracy of the device large-signal and IM_3 distortion characterization and the practicability of the proposed method are illustrated through comparison between measured and predicted results.**

I. INTRODUCTION

MICROWAVE AMPLIFIERS employing GaAs MESFET devices are used extensively in medium-power applications. Their suitability, especially for applications in multiple-carrier systems, depends on their output power, gain, and distortion performance. At present, no systematic procedure based on the device model for designing MESFET amplifiers for optimum large-signal power and intermodulation performance has been developed. It is believed that this is currently a general problem associated with the design of large-signal MESFET amplifiers.

One of the most powerful techniques for analyzing nonlinear circuits with mild nonlinearities is established to be that of the Volterra series representation [1]. Even though considerable work has been done in the area of MESFET power amplifiers using this series, most of the previously published work dealt only with the problem of third-order intermodulation distortion up to *S*-band frequencies [2], [3]. However, no further attempts have been made to predict the full power performance of MESFET amplifiers including both the optimum power and distortion performance. Other methods based on the modeling of the active device, by means of a nonlinear equivalent circuit have been employed to improve either the output power [4]–[6] or the intermodulation distortion [7], [8]. For example, Willing *et al.* [6] used a time-domain analysis to calculate the large-signal device characteristics. They obtained very good results, but the time-domain analysis is not very convenient for circuit design and is rather laborious. Also, Tucker [9] used a simple unilateral nonlinear circuit model to obtain the optimum loads for maximum intercept point and maximum output power. However, values of the device parameters which characterize the nonlinearities in the transistor were obtained from gain compression and IMD measurements. Perlow [10] took another approach in the prediction of the different types of third-order distortion, including intermodulation and gain compression. His technique relies on one type of distortion being known or estimating the gain compression. The method was independent of a specific device model and based on the transfer characteristics, both amplitude and phase, of the amplifier.

An alternative experimental approach to the design of FET amplifiers was employed by Sechi [11] to identify the optimum circuit load impedance for maximum output power at a predetermined value of intermodulation distortion and frequency. It was used for linear amplifiers and is based on load impedance contours for constant power and constant intermodualtion distortion. This method is, however, often inconvenient because contours were measured with the aid of a computer-controlled tuner which is complex in its setting up procedure, expensive, and time consuming. Additionally, for measurements of constant intermodulation contours, a degree of manual interaction is required.

This paper is divided into two parts. The first part investigates the full power and intermodulation performance of a single-stage amplifier at *X*-band. It is based on small-signal device measurements only in order to develop a nonlinear bilateral circuit model. A single- and two-tone input signal nonlinear analysis is capable of describing

Manuscript received March 20, 1985; revised May 24, 1985. This work was supported in part by Mullard, Ltd. This work was performed while the authors were with the Department of Electronics, Chelsea College, University of London.

G. M. Lambrianoa is with the Cyprus Telecommunication Authority, BOX 4929, Nicosia 142, Cyprus.

C. S. Aitchison is with ERA Technology Ltd., Cleeve Road, Leatherhead, Surrey, KT22 7SA, England.

0018-9480/85/1200-1395$01.00 ©1985 IEEE

with simple analytical expressions the amplifier performance. It is based on the Volterra series representation which includes interactions between the nonlinear parameters and spectrum components at harmonics and intermodulation frequencies. It is suitable for circuits with mild nonlinearities. Furthermore, a technique is developed to identify the dominant sources of gain compression and intermodulation distortion of the device embedded in an amplifier circuit. The analytical results are compared with measurements on an experimental GaAs MESFET amplifier at X-band.

The second part introduces a flexible procedure for the design of a large-signal MESFET amplifier which provides the best possible compromise in performance between output power and intermodulation distortion. The technique is supported from the results obtained in the first part. It uses the Volterra series nonlinear analysis results in order to relate the dependance of the output load to the output power and intermodulation distortion for any arbitrary input power level and at a fixed frequency. These are displayed in a suitable graphical form making the design process easy. Experimental verification of the method is given for two MESFET amplifiers with different load conditions; measured and predicted performances are compared.

II. MESFET Amplifier Nonlinear Model

The nonlinear circuit model of the amplifier employing a GaAs MESFET is shown in Fig. 1(a). The device is fed from a matched complex impedance Z_{ms} and is terminated with matched complex impedance Z_{mL}. The transistor model contains three nonlinearities, the gate to source capacitance C_g, the transconductance g_m, and the drain conductance g_0. The choice of the nonlinearities is based on typical published results [3], [4]. The nonlinearities have physical origins and are based both on physical models and measurements. The physical model is derived primarily from the JFET model of [12], [13] with the necessary modifications to represent the MESFET nonlinearity voltage dependent characteristics ($g_m - V_{GS}$ and $C_g - V_{GS}$ for constant V_{DS}, and $g_0 - V_{DS}$ for constant V_{GS}). The model provides accurate equations to describe the device voltage-current curves and their derivations. Small-signal measurements are carried out to conform to the theory referred to above. The transconductance g_m has been determined from the static I–V characteristics, the gate capacitance C_g, from CV-profile measurements, and the conductance g_0, from the technique suggested by Mo *et al.* [14]. The voltage dependence of the nonlinearities is represented by three term power series above the operating point [3, eqs. (1) and (2)].

The choice of the third-order Volterra series analysis requires that the nonlinear elements must be presented by nonlinear voltage-controlled current generators using the first three terms of the Taylor series expansion of the characteristics above the operating point [3, eqs. (4)–(6)]. The nonlinear current sources are superimposed on the linear circuit in the form of additional current generators

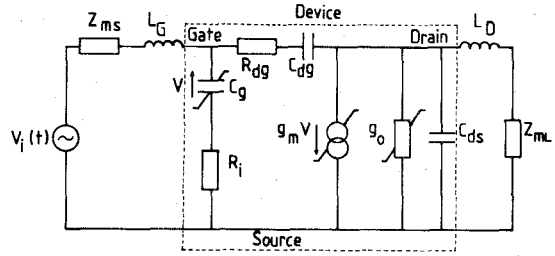

(a)

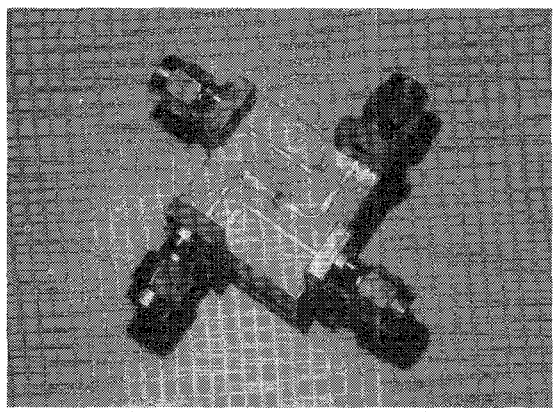

(b)

Fig. 1. (a) Nonlinear circuit representation of the MESFET amplifier under large signal conditions. Device element values: $R_i = 21\ \Omega$, $R_{dg} = 89\ \Omega$, $C_{dg} = 0.035$ pf, $C_{ds} = 0.09$ pf. Coefficient of the nonlinear current Taylor series: $g_{m1} = 0.0207$, $g_{m2} = 0.012$, $g_{m3} = -0.0033$, $C_{g1} = 0.41$E-12, $C_{g2} = 0.131$E-12, $C_{g3} = 0.045$E-12, $g_{01} = 0.836$E-3, $g_{02} = 0.252$E-3, $g_{03} = 0.033$E-3. (b) Internal view of one-stage conjugately matched amplifier at 7.8 GHz.

[2]. More details about the nonlinear circuit derivations are available in [3], where a nonlinear model suitable for the Volterra series analysis has been successfully obtained.

The GaAs MESFET used in all amplifiers is an experimental device with a 1.2×200-μm gate operated at bias voltages of $V_{GS} = 0.0$ V, $V_{DS} = 5$ V, and $I_D = 22$ mA. The MESFET optimized linear element values from measured S-parameters (2–12 GHz) together with the first three coefficients of the nonlinear current Taylor series are given in Fig. 1(a). L_G and L_D are inductances of bond wires of the gate and drain, respectively.

III. Nonlinear Analysis of the MESFET Amplifier

The summary of the power and intermodulation distortion analysis of the MESFET amplifier is given below. Consider an input signal into an amplifier (as shown in Fig. 1(a)) consisting of two equal amplitude sinusoidal signals at the incommensurable frequencies ω_1 and ω_2 as

$$V_i(t) = v_i(\cos \omega_1 t + \cos \omega_2 t). \tag{1}$$

The source and load impedances of the nonlinear circuit have real and imaginary parts given by

$$Z_{ms} = R_s + jX_s \tag{2}$$

$$Z_{mL} = R_L + jX_L. \tag{3}$$

Based on the Volterra series analysis [1], the output voltage component at frequency ω_1 is

$$v_i H_1(\omega_1)+3/4 v_i^3 H_3(\omega_1,\omega_1,-\omega_1) +3/2 v_i^3 H_3(\omega_1,\omega_2,-\omega_2)+\cdots$$

where $H_1(\omega_1)$ is the circuit linear transfer function, while $H_3(\omega_1,\omega_1,-\omega_1)$ and $H_3(\omega_1,\omega_2,-\omega_2)$ are the circuit nonlinear transfer functions or Volterra kernels, and can be calculated utilizing the technique described in [1] and [15]. For computation convenience, it can be assumed that

$$H_1(\omega_1)\simeq H_1(\omega_2)\triangleq H_1(\omega_0)$$

and

$$H_3(\omega_1,\omega_1,-\omega_1)\simeq H_3(\omega_1,\omega_2,-\omega_2)\triangleq H_3(\omega_0,\omega_0,-\omega_0)$$

because, in practice, the two-tone measurements of an amplifier occur when the frequency separation between the two exciting input signals is a few megahertz. With this assumption, the output components at frequency ω_1 can be rewritten in a more general form, covering, additionally, the case for single-input signal excitation, as

$$v_i H_1(\omega_0)+3\left(\frac{2N-1}{4}\right)v_i^3 H_3(\omega_0,\omega_0,-\omega_0)+\cdots, \qquad N=1,2 \quad (4)$$

where N represents the number of exciting input signals. From (4), the circuit nonlinear transfer function for single- or two-tone input signals, $T_{NL}(\omega_0)$ may be expressed in terms of amplifier Volterra kernels or transfer functions and the available input power as

$$T_{NL}(\omega_0)=H_1(\omega_0)+3(2N-1)P_{av}(\omega_0)\mathrm{Re}[Z_{ms}]\cdot H_3(\omega_0,\omega_0,-\omega_0)+\cdots, \qquad N=1,2 \quad (5)$$

where

$$P_{av}(\omega_0)=\frac{|v_i|^2}{4\mathrm{Re}[Z_{ms}]}$$

is the available input power. Also, the nonlinear output power at ω_0, $P_{ONL}(\omega_0)$, can be expressed as

$$P_{ONL}(\omega_0)=\frac{|V_{ONL}(\omega_0)|^2}{\mathrm{Re}[Z_{mL}]} \quad (6)$$

where $V_{ONL}(\omega_0)$ is the output voltage across the real part of the matched-load Z_{mL}. Using (5) and (6), the amplifier nonlinear power gain for single- and double-input signals at ω_0, $G_{NLP}(\omega_0)$ in decibels is given by

$$G_{PNL}(\omega_0)=10\log_{10}|T_{NL}(\omega_0)|^2 +10\log_{10}\left|\frac{R_L}{R_L+jX_L(\omega_0)}\right|^2 +10\log_{10}\left|4\cdot\mathrm{Re}\left\{\frac{Z_{ms}}{Z_{mL}}\right\}\right|. \quad (7)$$

It can be seen from (7) that the nonlinear output power for a single- or double-input signal at ω_0 is of the form

$$P_{ONL}(\omega_0)=G_{PNL}(\omega_0)\cdot P_{av}(\omega_0). \quad (8)$$

Equations (7) and (8) express the nonlinear power gain and the output power for single- or two-tone input signals, as a function of the amplifier nonlinear transfer functions, the input frequency, and the terminated loads, for any arbitrary input power level.

The third-order intermodulation distortion (IM_3) is defined as the ratio of the distortion output power at $2\omega_1-\omega_2$ or $2\omega_2-\omega_1$ to the fundamental frequency power at ω_1 in the output load impedance. The third-order intermodulation output at $2\omega_1-\omega_2$ is calculated from the Volterra series as

$$3/4 v_i^3 H_3(\omega_1,\omega_1,-\omega_2).$$

Following the same procedure as in the case of the fundamental output power $P_{ONL}(\omega_0)$, the output power at $2\omega_1-\omega_2$, $P_{ONL3}(\omega_0)$, in decibels, may be expressed in terms of the amplifier transfer function and the available input power as

$$P_{ONL3}(\omega_0) =20\log_{10}|3P_{av}(\omega_0)\mathrm{Re}[Z_{ms}]H_3(\omega_0,\omega_0,-\omega_0)| +20\log_{10}\left|\frac{R_L}{R_L+jX_L(\omega_0)}\right| +10\log_{10}\left|4\mathrm{Re}\left\{\frac{Z_{ms}}{Z_{mL}}\right\}\right| +10\log_{10}|P_{av}(\omega_0)|. \quad (9)$$

The compression of the output power is the next parameter for discussion. By definition, the voltage compression ratio $K(\omega_0)$ is the deviation of the amplifier voltage gain from its small-signal value [4]. This is derived from (5) and (6) for both the single- and two-tone input signals as

$$|K(\omega_0)|\simeq 1+\frac{3(2N-1)}{4}P_{av}(\omega_0)\cdot\mathrm{Re}[Z_{ms}]\cdot\mathrm{Re}\left\{\frac{H_3(\omega_0,\omega_0,-\omega_0)}{H_1(\omega_0)}\right\}, \qquad \text{for } N=1,2. \quad (10)$$

In terms of power gain, the corresponding parameter is $|K(\omega_0)|^2$ and is called the gain compression factor. It is expressed as a function of the amplifier nonlinear transfer functions, the input frequency, and the terminated loads, for any arbitrary input power level.

The theory presented so far is subject to a limitation which can be derived from (8) and (10) and is found in the form of the following inequality:

$$\frac{\mathrm{Re}\left\{\frac{H_1(\omega_0)}{H_3(\omega_0,\omega_0,-\omega_0)}\right\}}{3(2N-1)\mathrm{Re}[Z_{ms}]}\geq P_{av}(\omega_0)\geq 0, \qquad \text{for } N=1,2. \quad (11)$$

The last equation gives the range of the input power for

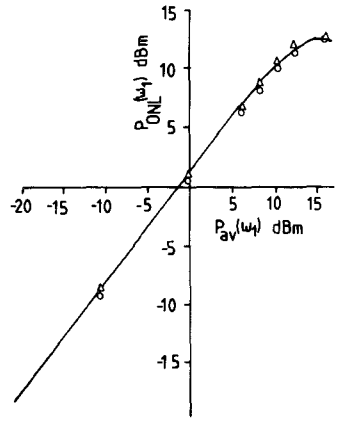

Fig. 2. Comparison between calculated and measured single-tone output power versus input power for the device between 50-Ω load input–output microstrip lines at 7.8 GHz. ——: Calculated from computer. ∘: Calculated from Volterra series. △: Measured.

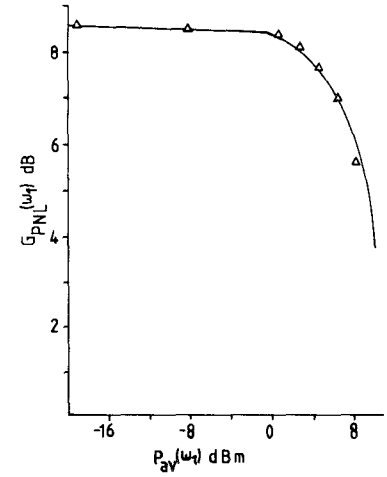

Fig. 4. Calculated and measured single-tone output power gain versus input power at 7.8 GHz. ——: Calculated using Volterra Series. △: Measured.

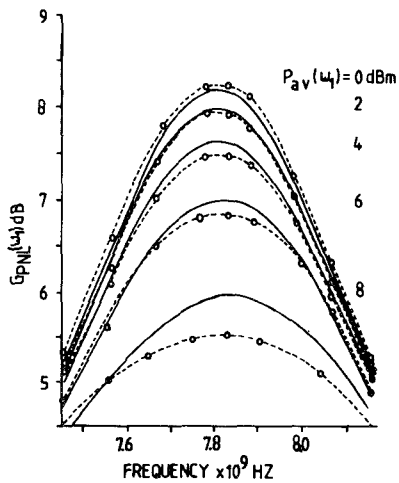

Fig. 3. Comparison between calculated and measured single-tone power gain frequency response for a conjugated match amplifier for different input power level at 7.8 GHz. ——: Calculated using Volterra Series. -- ∘ --: Measured.

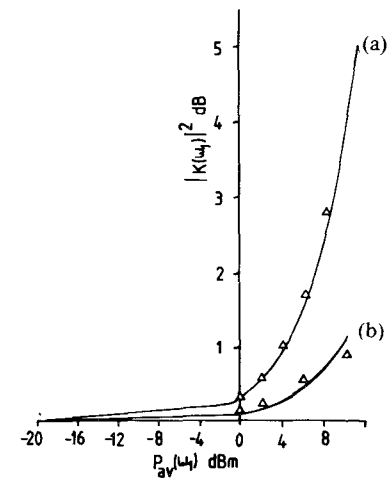

Fig. 5. Calculated and measured gain compression at 7.8 GHz (a) for the conjugated match amplifier and (b) for the device between 50-Ω input–output microstrip lines. ——: Calculated. △: Measured.

single- and two-tone input signals where the theory is valid. It is seen that it is a function of the input power and device parameters.

IV. Experimental Verification

Two experimental tests were carried out in order to compare measured and predicted amplifier power and intermodulation performance. The first experimental test has two objectives. Firstly, to demonstrate the advantage of frequency-domain analysis over the time-domain analysis, and secondly, to compare the results of the frequency-domain analysis using the Volterra series with the time-domain analysis using the computer program SPICE 2. Fig. 2 shows the comparison between calculated (time and frequency domain) and measured, single-tone output power versus input power for a 7.8-GHz amplifier consisting of MESFET device between 50-Ω input–output microstrip lines. It should be noted that the calculation of the output power using SPICE 2 involves excessive computer time. This is much slower than the direct method using the Volterra series in the frequency domain, which calculates the response directly.

The next experimental test is to fully measure and predict the power and intermodulation performance of an amplifier with single- and two-tone input test signals. A conjugately matched amplifier built on an alumina substrate using quarter-wave matching sections is employed for this experiment and is shown in Fig. 1(b). Fig. 3 shows the measured and calculated nonlinear power gain as a function of the input frequency for different input power levels. Fig. 4 presents the calculated and measured results of the nonlinear power gain as a function of the input power. Fig. 5 shows the gain compression curves for both the conjugate match and 50-Ω load amplifier as a function of the input power. The intermodulation performance of the amplifier is shown in Fig. 6. The frequency separation of the two-tone input signal is 5 MHz. Fig. 6 illustrates the fundamental frequency and third-order intermodulation

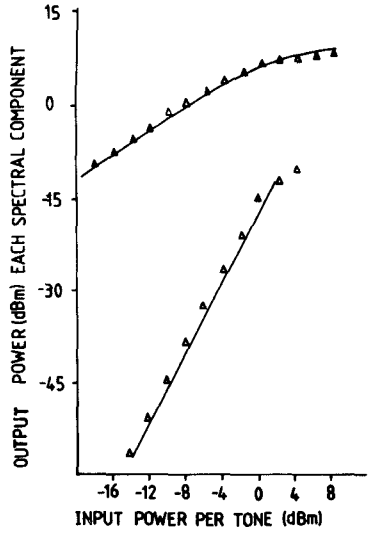

Fig. 6. Calculated and measured fundamental output and intermodulation distortion versus input power per tone at 7.8 GHz. $\Delta f = 5$ MHz. Δ: Measured. ——: Calculated.

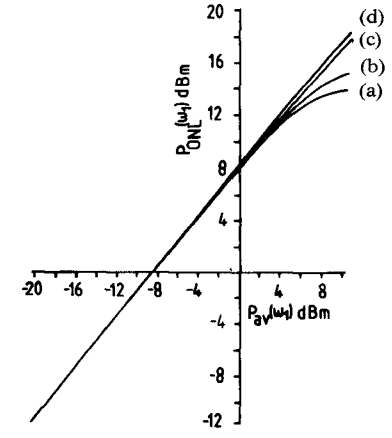

Fig. 7. Calculated single-tone output power versus input power for the conjugated match amplifier at 7.8 GHz (a) including all nonlinearities, (b) including g_0 nonlinearity only, (c) including g_m nonlinearity only, (d) including C_g nonlinearity only.

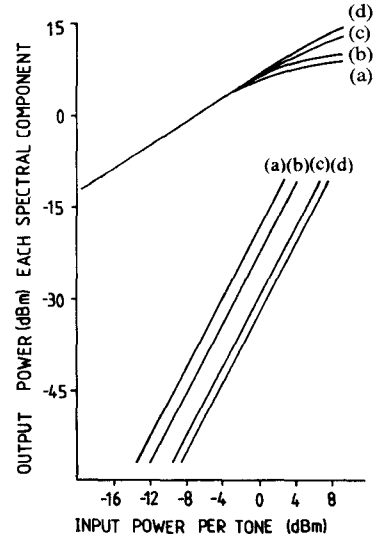

Fig. 8. Calculated two-tone fundamental output and intermodulation distortion versus input power per tone at 7.8 GHz (a) including all nonlinearities, (b) including g_0 nonlinearity only, (c) including g_m nonlinearity only, (d) including C_g nonlinearity only.

frequency output power as a function of the input power per tone at 7.8 GHz for the conjugate match amplifier. Figs. 2–5 serve to demonstrate the ability of the model in conjunction with the theory to predict the large-signal performance of an amplifier for single-tone input signal from small-signal measurements. Measured and predicted points using the nonlinear model are substantially coincident, although small discrepancies with a maximum of 0.5 dB at higher input power levels are observed. The ability of the theoretical model to predict the distortion performance of the amplifier for a two-tone input signal is demonstrated in Fig. 6. Although measured and predicted results are in good agreement, small deviations of the measured results at higher input power levels occur, as in the case of the single-tone test, and may be due to the contribution of higher order transfer functions which are not included in this analysis. However, the general dependance of the model on nonlinearities, termination impedances, and input power levels (single and two tones) is successfully represented. The limitations, given in (11), imposed on the input power level for this particular device, were calculated using (11) to permit approximately 10 and 7 dBm for a single- and double-input signal levels, respectively.

Having taken into account the total effect of all the nonlinearities, it is now relevant to examine their individual effects in both the power and distortion performance of the amplifier. Since these effects are not separately measurable, the relative contribution made by each nonlinearity can be assessed by including the nonlinear elements one at a time in the nonlinear model and computing the input–output power characteristics for the single-tone test, and the IM_3 characteristics for the double-tone test. The results for the conjugate match amplifier under a single-tone input signal are presented in Fig. 7. The conductance g_0 is the dominant nonlinearity for a single-tone signal, which compresses the output power from its linear value by 3.7 dB; next the transconductance g_m (with a smaller effect) by 0.93 dB, and, finally, the C_g capacitance, with an almost negligible effect of 0.35 dB, with 10-dBm input power. Similarly, the corresponding results for two-tone input signal are illustrated in Fig. 8. These results show that g_0 is again the dominant nonlinearity which improves the IM_3 from its measured value by 5 dB, followed by g_m with higher effect by 13 dB and C_g by 16 dB with -5-dBm input power. Also, this figure demonstrates results similar to those of Fig. 7 for the output compression but with a two-tone input signal where output power saturates 3 dB lower. The behavior of the nonlinearities suggest that the device output power and distortion performance is sensitive to load impedance and relatively insensitive to source impedance. Therefore, load impedance may be used to substantially control the power and intermodulation performance of the amplifier.

V. A Design Procedure for Optimum Large-Signal Power and IM_3 Distortion Performance

The results due to the previous device characterization verify that:

i) the device nonlinear model can be accurately represented by three nonlinearities;
ii) the nonlinear model in conjunction with the Volterra series representation can predict the power and distortion performance of the amplifier under different input power and load conditions with the aid of a simple computer program;
iii) the device power and distortion performance are sensitive only to load impedance.

It is the objective of this program to develop a method for the design of a MESFET amplifier under large-signal conditions, based on these characterization results. The method is capable of determining a set of design parameters in a suitable graphical form which result in the choice of the optimum load impedance for the best compromise between the output power and IM_3 distortion. First, we describe the procedure for this design, followed by the experimental verifications by means of two MESFET amplifiers with various load conditions.

A. Design Procedure

The nonlinear MESFET equivalent-circuit configuration used for the design procedure is shown in Fig. 1(a). The most important external parameters are the load impedance and the input power level. It has been shown that different load impedances are required in order to obtain either minimum intermodulation distortion or maximum saturation output power or maximum gain [11]. Therefore, the load impedance of the model Z_{mL} is chosen as a variable and, with the aid of computation, a device characterization is accomplished. This characterization indicates how the output power and IM_3 distortion vary as a function of the load impedance. The model load impedance consists of a 50-Ω microstrip line of variable electrical length, in series with a quarter-wave transformer of variable characteristic impedances. These variables can produce any desired combination of load impedance. Then a computer program based on the third-order Volterra series analysis was developed to calculate the value of a load impedance which produces the fundamental output power and the corresponding carrier to intermodulation (C/I) ratio for a two-tone input at a fixed frequency; this is repeated for various input power levels. In all cases, the input was matched for maximum gain based on the previous characterization. Using this information, two 8-GHz amplifiers were designed. The first, amplifier A, is a small-signal maximum gain amplifier and is used as a comparison for amplifier B. Amplifier B is designed for the optimum load impedance which gives the best performance between output power and IM_3 under large-signal conditions.

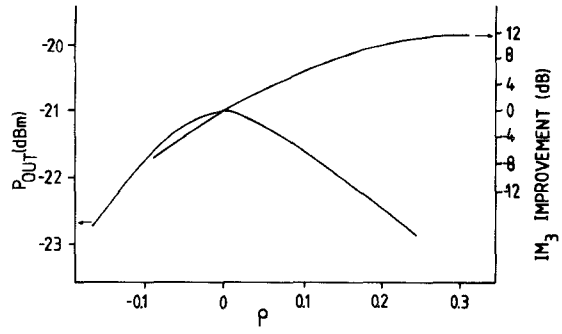

Fig. 9. Calculated power and IM_3 improvement versus load impedance at $f = 8$ GHz and $P_{IN} = -30$ dBm. Key: $\theta = -102°$ for $\rho < 0$. $\theta = -75°$ for $\rho > 0$.

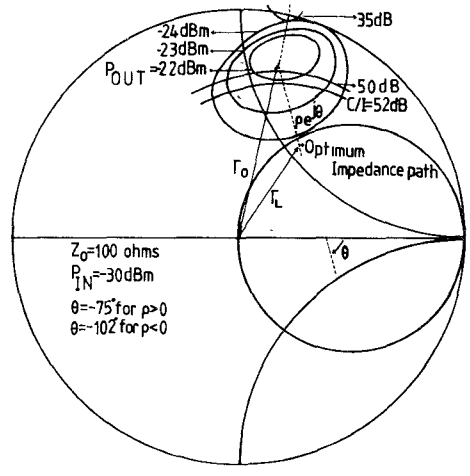

Fig. 10. Calculated contours of constant output and C/I. $Z_0 = 100$ Ω, $f = 8$ GHz, and $P_{IN} = -30$ dBm.

1) Design of the Amplifier A: The variation of the fundamental frequency output power and the corresponding improvement in IM_3 product with the input power and frequency as constant parameters have been computed as a function of the load impedance, and are illustrated in Fig. 9. The load impedance is a function of a real variable ρ, and can be expressed [11] in terms of its reflection coefficient as is represented graphically in Fig. 10

$$\Gamma_L = \Gamma_0 + \rho e^{j\theta}$$

where Γ_0 is the reflection coefficient of the load impedance for maximum output power, Γ_L is the reflection coefficient of any impedance along the graph, ρ is equal to $|\Gamma_L - \Gamma_0|$, and θ is the angular position of ρ with respect to Γ_0. The output power curve defines the values of load impedances which produce the maximum value of fundamental frequency output power per tone at operating conditions. The IM_3 improvement curve is extracted from the computed C/I ratio normalized to the maximum output power condition. Both the output power and IM_3 improvement values correspond to the unique set of load impedances as given by Fig. 9. This condition is obtained utilizing the technique described in [11] as shown in Fig. 10. The same figure demonstrates the optimum impedance path which provides the maximum output power for the corresponding

value of C/I. It is defined as the locus of the tangent points between the power and C/I contours. This is well explained in [11].

The input power level for this design is chosen to lie in the amplifier's linear operating region (−30 dBm). This amplifier is designed to give maximum gain rather than a particular IM_3 performance. The output load corresponding to maximum gain is $25 + j127.5$. A conjugately matched amplifier was built on an alumina substrate, with this output load in the form of quarter-wave matching sections.

2) Design of Amplifier B: Amplifier B, which operates under large-signal conditions, is designed to reduce the IM_3 product while allowing a small reduction in output power. The design proceeds in four steps.

Step 1. Select the input power level for the design. The third-order Volterra series analysis predicts a 3:1 increase in the intermodulation level with an input power increase. In practice, deviation from this slope occurs at high signal levels, especially in the saturation region; however, the analysis is able to accurately predict this behavior in the compression region. In this region, the various nonlinear distortion effects begin to become significant. Therefore, the input power level is chosen to lie in the amplifier's gain compression region (0 dBm for two-tone signal).

Step 2. Obtain the amplifier load impedance for maximum output power. The device characterization data, due to computer prediction, for an input of 0 dBm at 8 GHz is shown in Fig. 11. Following the same procedure as in the case of amplifier A, this set of optimum load impedance values is obtained from Fig. 12. The output power curve defines the unique value of load impedance which produces the maximum value of output power per tone at the operating condition. The maximum of this curve gives the optimum load impedance for maximum output power under the specified conditions. It can be observed that the maximum gain is lower than in the case of amplifier A, as would be expected.

Step 3. Calculate the IM_3 improvement under maximum load conditions. Previous observation confirms that if the output is mismatched either to give less than optimum gain in the linear region or optimum output power at the nonlinear region, then a particular mismatch exists which minimizes intermodulation distortion [16]. In the present characterization, the mismatch required for the maximum output power results in some improvement for the amplifier under large-signal conditions (point 0, Fig. 11). The IM_3 improvement curve scale is normalized to point 0, and the rest of the points can then be plotted from the C/I ratio calculated from the computer program results. It can be seen that the load impedance for maximum output power provides an additional 5-dB IM_3 improvement calculated at 0-dBm input power for the corresponding load conditions of the two amplifiers.

Step 4. Choice of the optimum load impedance for the best performance. It can be seen by inspection of Fig. 11 that along a curve of IM_3 improvement, the optimum load impedance for maximum output power and IM_3 improvement lie at the intersection of the two curves. The choice of

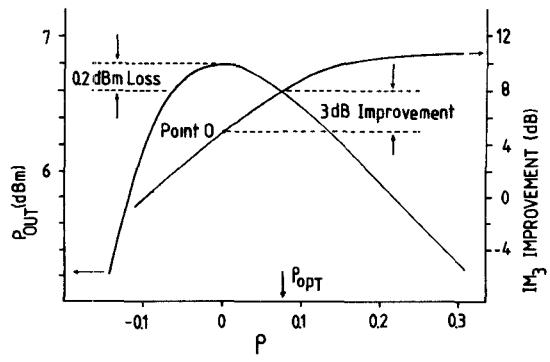

Fig. 11. Calculated power and IM_3 improvement versus load impedance at $f = 8$ GHz and $P_{IN} = 0$ dBm. Key: $\theta = -78°$ for $\rho < 0$. $\theta = -96°$ for $\rho > 0$.

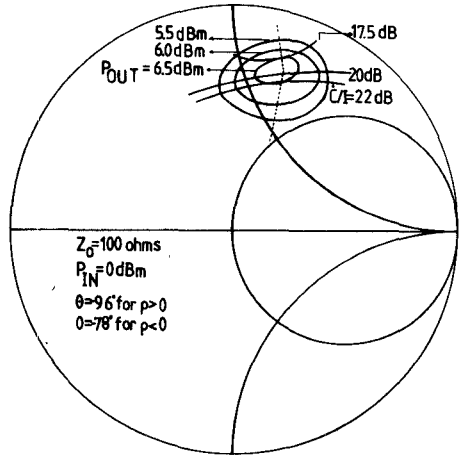

Fig. 12. Calculated contours of constant output power and C/I at $f = 8$ GHz and $P_{IN} = 0$ dBm.

the optimum load impedance is based on the behavior of the IM_3 improvement curve together with the output power characteristic. The same figure shows that the IM_3 improvement curve increases linearly and positively in the region $+0.1 \geq \rho \geq -0.1$. Above this region, the curve begins to saturate and the IM_3 improvement is negligible in comparison with the output power reduction. The selection of an operating load which corresponds to ρ_{opt} gives an extra 3-dB improvement in IM_3, in the compression region at the expense of only 0.2 dBm in the output power. The optimum load impedance value obtained at 8 GHz is $48 + j122$. The output of amplifier B was designed for this impedance and its construction is similar to amplifier A.

B. Experimental Verification

An accurate large-signal model forms the foundation of the proposed method. The method is capable of deriving the optimum load conditions for the amplifier best performance. Once the optimum load has been obtained, the design of the small- or large-signal amplifier is a simple linear design routine. As outlined in the previous section, the input and output matching networks of both amplifiers are composed of quarter-wave matching sections.

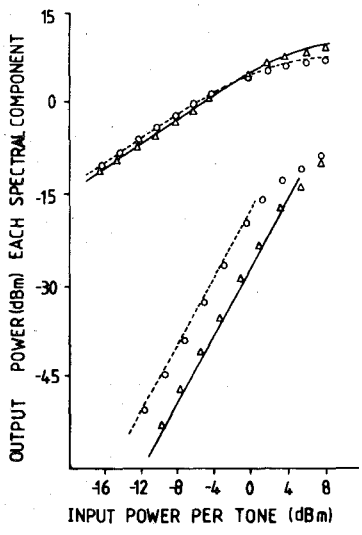

Fig. 13. Calculated and measured fundamental output power and intermodulation distortion versus input power per tone at 8 GHz, $\Delta f = 5$ MHz for amplifiers A and B. ----: Calculated, ∘: Measured for amplifier A. ——: Calculated, Δ: Measured for amplifier B.

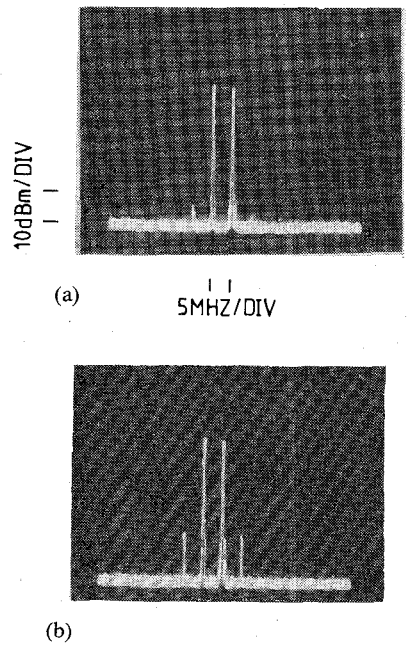

Fig. 14. Signal spectrum of the output of the amplifier A and B at $P_{IN} = -10$ dBm. (a) Amplifier B, (b) Amplifier A. Vertical scale 10 dB/division; horizontal 5 MHz/division.

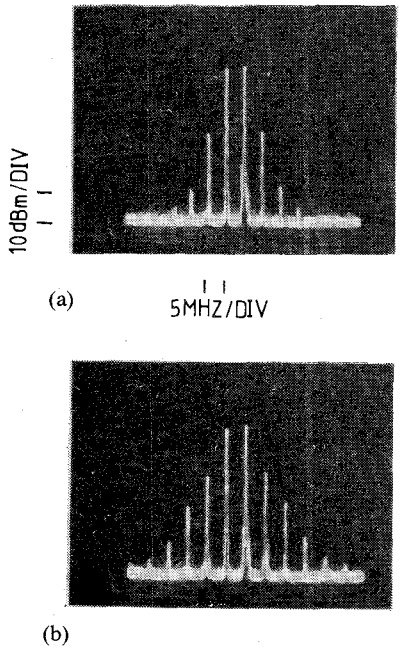

Fig. 15. Signal spectrum of the output of the amplifier A and B at $P_{IN} = 2$ dBm. (a) Amplifier B, (b) Amplifier A. Vertical scale 10 dB/division; horizontal 5 MHz/division.

The theoretical and experimental performance of amplifiers A and B are demonstrated in Fig. 13. It shows the fundamental and IM_3 frequency output power as a function of the input power per tone at 8 GHz for the two amplifiers both in theory and practice. The frequency separation of the two-tone input signal is 5 MHz. The improvement of output power per tone at the fundamental frequency in the saturation region in amplifier B was measured to be 2 dB greater than amplifier A at 7-dBm input power. However, the corresponding reduction in output power in the linear region is only 0.9 dB. The theoretical predictions were approximately 2 dB and 0.8 dB, respectively. The spectrums' pictures at the output of the amplifier A and B at input power -10 and 0 dBm are shown in Figs. 14 and 15, respectively, for a two-tone input signal. For a -10-dBm input power per tone, the improvement in the IM_3 product is 8.5 dB in amplifier B compared with that of amplifier A, while for a 2-dBm input power per tone the improvement is 5.2 dB. In general, the agreement between the predicted and measured performance is good. The small discrepancies at higher input power levels are attributed to contributions from higher order transfer functions which are not included in this computer program. However, the general dependance of small-signal gain, saturation power, and IM_3 products on termination impedance and input power is successfully simulated.

The experimental results of the two amplifiers quantatively illustrate that the optimum out of band mismatches results in a decrease of the amplifier output power and IM_3 product in both the linear and nonlinear regions. However, the IM_3 reduces significantly in comparison with a negligible loss of output power, resulting in a net improvement in both IM_3 distortion and output power on comparison with an optimum gain amplifier. It should be noted that this design procedure can be applied to different input frequencies inside the device model frequency range.

Finally, this procedure gives directly the optimum load impedance for designing MESFET amplifiers for optimum large-signal power performance without the necessity of plotting constant power contours.

VI. Conclusion

A third-order nonlinear analysis of a GaAs MESFET amplifier based on the device nonlinear model and using the Volterra series has been developed. The principal ad-

vantages of this analysis are the simplicity in predicting single- and double-output power and IM_3 distortion response and the fact that it requires only small-signal measurements of the device. The favorable agreement between theory and experimental single-stage amplifier results confirmed the validity of this characterization. Furthermore, the model in conjunction with theory is useful in identifying the major causes of gain compression and IM_3 distortion of the device in an amplifier.

A systematic procedure has been proposed and obtained for designing MESFET amplifiers for the best compromise between output power and IM_3 distortion performance. The theoretical and experimental comparison of the two amplifiers confirmed that the optimum out of band matching offers a distinct power linearity and IM_3 improvement and seals the validity of the method. The important merit of the method is that it fully relies on small-signal measurements only. This technique may be applied to replace the tedious and expensive load-pull technique and it may find applications in oscillators design.

Acknowledgment

The authors would like to thank Dr. C. Camacho-Penalosa of the Universidad Politechina de Madrid, Spain, for helpful discussions.

References

[1] J. Bussgang, L. Ehrman, and J. Craham, "Analysis of nonlinear systems with multiple inputs," *Proc. IEEE*, vol. 62, pp. 1089–1119, Aug. 1974.

[2] A. M. Khadr and R. H. Johnston, "Distortion in high frequencies amplifiers," *IEEE Solid-State Circuits*, vol. SC-9, pp. 180–189, Aug. 1974.

[3] R. A. Minasian, "Intermodulation distortion analysis of MESFET amplifier using Volterra series representation," *IEEE Trans. Microwave Theory Tech.*, vol. MTT-28, pp. 1–8, Jan. 1980.

[4] R. S. Tucker, "RF characterisation of microwave power FET's," *IEEE Trans. Microwave Theory Tech.*, vol. MTT-29, pp. 776–781, Aug. 1981.

[5] Y. Tajima, Y. B. Wrona, and K. Yishima, "GaAs FET large-signal model and its application to circuit designs," *IEEE Trans. Electron Devices*, vol. ED-28, pp. 171–175, Feb. 1981.

[6] H. A. Willing, C. Rauscher, and P. de Santis, "A technique for predicting large-signal performance of a GaAs MESFET," *IEEE Trans. Microwave Theory Tech.*, vol. MTT-26, pp. 1017–1023, Dec. 1978.

[7] J. A. Higgins and D. L. Kuvas, "Analysis and improvement of intermodulation distortion in GaAs power FET's," *IEEE Trans. Microwave Theory Tech.*, vol. MTT-28, pp. 9–17, Jan. 1980.

[8] R. A. Pucel, "Profile design for distortion reduction in microwave field-effect transistor," *Electron. Lett.*, vol. 14, pp. 204–206, Mar. 1978.

[9] R. S. Tucker, "Third-order intermodulation distortion and gain compression in GaAs FETs," *IEEE Trans. Microwave Theory Tech.*, vol. MTT-27, pp. 400–408, May 1979.

[10] S. M. Perlow, "Third-order distortion in amplifiers and mixers," *RCA Rev.*, vol. 37, pp. 234–266, June 1976.

[11] N. F. Sechi, "Design procedure for high efficiency linear microwave power amplifiers," *IEEE Trans. Microwave Theory Tech.*, vol. MTT-28, pp. 1157–1163, Nov. 1980.

[12] T. S. Nashashibi, "A JFET model," *Thorn EMI PLC*, Aug. 1982.

[13] R. S. Cobbold, *Theory and Application of Field-Effect Transistors*. New York: Wiley Interscience, 1970, pp. 75–76.

[14] D. L. Mo and H. Yanai, "Current voltage characteristics of the junction gate FET with field dependance mobility," *IEEE Trans. Electron Devices*, vol. ED-17, pp. 577–586, Aug. 1970.

[15] E. Bedrosian and S. O. Rice, "The output properties of Volterra System (nonlinear system with memory) driven by harmonic and Gausian inputs," *Proc. IEEE*, vol. 59, pp. 1688–1707, Dec. 1971.

[16] B. Dorman, W. Slusark, Jr., Y. S. Wu, P. Pelka, R. Barton, H. Wolkstein, and H. Huang, "A 4-GHz GaAs FET power amplifier: An advanced transmitter for satellite down-link communication systems," *RCA Rev.*, vol. 41, pp. 472–503, Sept. 1980.

George M. Lambrianou was born in Galata, Cyprus, in October 1956. He received the B.Sc.(Eng) degree in electronic engineering from Chelsea College, London University, in 1982. From 1982 to the summer of 1985, he was working towards the Ph.D. degree in the area of nonlinear microwave amplifiers, in the same college.

Since the summer of 1985, he has been employed by the Cyprus Telecommunication Authority. His interests are in the area of nonlinear microwave amplifiers and their applications on satellite communication.

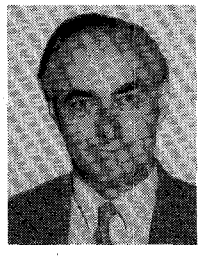

Colin S. Aitchison was born in Morecambe, England, in 1933. He received the B.Sc. and A.R.C.S. degrees in physics from Imperial College, London, England, in 1955.

He worked for Philips Research Laboratories, Redhill, Surrey, England, from 1955 to 1972, being initially concerned with the noise-reduction properties of direct injection phase-locked klystrons for use with Doppler radars. He led a group concerned with parametric amplifiers, mixers, ferrite limiters, lumped microwave components, and Gunn and avalanche oscillators. In 1972, he joined the Department of Electronics, Chelsea College, University of London, London, England, where he was Professor in Electronics. In 1982, he joined ERA Technology, Ltd. His research interests remain in the field of active microwave circuits, particularly distributed amplifiers.

Prof. Aitchison is a Fellow of the Institution of Electrical Engineers, a Member of the Institute of Physics, and an Emeritus Professor of the University of London.